International Journal for Modern Trends in Science and Technology, 8(06): 632-640, 2022

ISSN: 2455-3778 online
DOI: https://doi.org/10.46501/IJMTST0806106
Available online at: http://www.ijmtst.com/vol8issue06.html

Lung and Pancreatic Tumor Characterization using Supervised and Unsupervised Deep Learning Approaches

Antony Asir Daniel[1] | Maria Jesi[2]

[1]Electronics and Communication Engineering, Loyola Institute of Technology and Science, Nagercoil, Tamilnadu, India
[2]Computer Science and Engineering, Loyola Institute of Technology and Science, Nagercoil, Tamilnadu, India

To Cite this Article
Antony Asir Daniel and Maria Jesi. Lung and Pancreatic Tumor Characterization using Supervised and Unsupervised Deep Learning Approaches. International Journal for Modern Trends in Science and Technology 2022, 8(06), pp. 632-640. https://doi.org/10.46501/IJMTST0806106

Article Info
Received: 12 May 2022; Accepted: 10 June 2022; Published: 27 June 2022.

ABSTRACT

Lung and Pancreatic tumors are the two common cancers in the world. Characterization of tumors from radiology images is more accurate and faster with computer-aided diagnosis (CAD) tools. Tumor Characterization through CAD tools enable non-invasive cancer staging, prognosis and foster personalized treatment planning for precise medicine. In this work, both supervised and unsupervised machine learning approaches are proposed to improve tumor characterization. The accuracy of about 97.6 % is obtained. This has proved that this would be the best method to characterize the tumor to diagnose the malignancy giving the better treatment for cancer survivors.

KEYWORDS: Computer Aided Designing (CAD), Artificial Neural Network (ANN), Computed Tomography (CT), Convolutional Neural Network (CNN), Magnetic Resonance Imaging (MRI), Learning from Label Proportion (LLP), Multi Task Learning (MTL), High Resolution Computed Tomography (HRCT), Fully Convolutional Network (FCN).

1. INTRODUCTION

Cancer is the number-one cause of deaths in the world. Out of 8.2 million deaths due to cancer worldwide, lung cancer accounts for the highest number of mortalities i.e. 1.59 million. Risk stratification of lung nodules can aid in identifying cancer stage leading to improved treatment and higher chances of survival. In addition, any significant development to accurately and automatically characterize lung nodules can save significant manual exertion as well as valuable time.

Lung Cancer:

Some of the most malignant tumors found among the cancer survivors are lung and pancreatic tumors. The lung cancer has found to be the most common cancer all over the world. Early diagnosis is one of the ways to reduce deaths related to lung cancer. In this regard, lung screening programs are especially beneficial. Low Dose Computed Tomography (CT) scans are usually used to perform lung nodule diagnosis, including both detection and risk stratification. Although CT imaging remains the gold standard for lung cancer detection and diagnosis, Computer-Aided Diagnosis (CAD) and quantification tools are often necessary. Moreover, research in

developing CAD algorithms can help explore the domain of imaging features and biomarkers which can be then studied by radiologists to further improve clinical decision making.

Avoidance of risk factors, including smoking and air pollution, is the primary method of prevention. Treatment and long-term outcomes depend on the type of cancer, the stage (degree of spread), and the person's overall health. Most cases are not curable. Common treatments include surgery, chemotherapy, and radiotherapy. NSCLC is sometimes treated with surgery, whereas SCLC usually responds better to chemotherapy and radiotherapy.

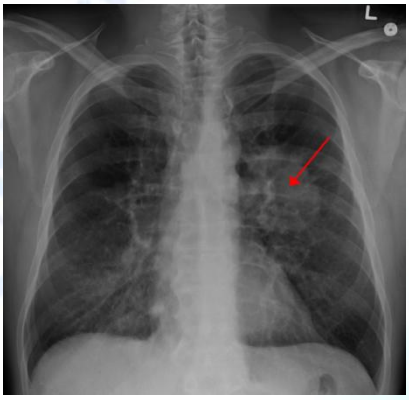

Fig.1.Lung Cancer

Worldwide in 2012, lung cancer occurred in 1.8 million people and resulted in 1.6 million deaths. This makes it the most common cause of cancer-related death in men and second most common in women after breast cancer. The most common age at diagnosis is 70 years.

Signs and symptoms which may suggest lung cancer include:[1]

- Respiratory symptoms: coughing, coughing up blood, wheezing, or shortness of breath
- Systemic symptoms: weight loss, weakness, fever, or clubbing of the fingernails
- Symptoms due to the cancer mass pressing on adjacent structures: chest pain, bone pain, superior vena cava obstruction, or difficulty swallowing

If the cancer grows in the airways, it may obstruct airflow, causing breathing difficulties. The obstruction can also lead to accumulation of secretions behind the blockage, and increase the risk of pneumonia.

Pancreatic tumor:

Pancreatic cancer arises when cells in the pancreas, a glandular organ behind the stomach, begin to multiply out of control and form a mass. These cancerous cells have the ability to invade other parts of the body. There are a number of types of pancreatic cancer. The most common, pancreatic adenocarcinoma, accounts for about 85% of cases, and the term "pancreatic cancer" is sometimes used to refer only to that type.

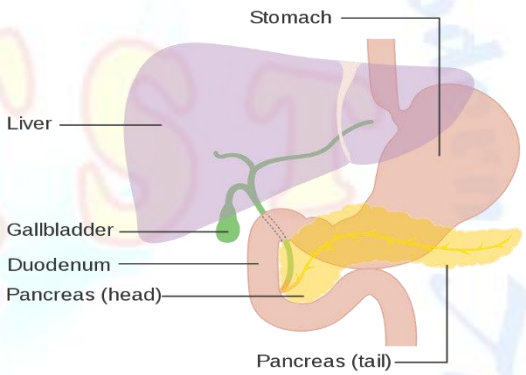

Fig.2.Pancreatic Cancer

These adenocarcinomas start within the part of the pancreas which makes digestive enzymes. Several other types of cancer, which collectively represent the majority of the non-adenocarcinomas, can also arise from these cells. One to two percent of cases of pancreatic cancer are neuroendocrine tumors, which arise from the hormone-producing cells of the pancreas. These are generally less aggressive than pancreatic adenocarcinoma.

In 2015, pancreatic cancers of all types resulted in 411,600 deaths globally.[10] Pancreatic cancer is the fifth most-common cause of death from cancer in the United Kingdom, and the third most-common in the United States. The disease occurs most often in the developed world, where about 70% of the new cases in

2012 originated. Pancreatic adenocarcinoma typically has a very poor prognosis: after diagnosis, 25% of people survive one year and 5% live for five years. For cancers diagnosed early, the five-year survival rate rises to about 20%. Neuroendocrine cancers have better outcomes; at five years from diagnosis, 65% of those diagnosed are living, though survival varies considerably depending on the type of tumor.

Digital image processing is the use of computer algorithms to perform image processing on digital images. As a subcategory or field of digital signal processing, digital image processing has many advantages over analog image processing. It allows a much wider range of algorithms to be applied to the input data and can avoid problems such as the build-up of noise and signal digital image processing may be modeled in the form of Multidimensional Systems.

One of the biggest advantages of digital imaging is the ability of the operator to post-process the image. Post-processing of the image allows the operator to manipulate the pixel shades to correct image density and contrast, as well as perform other processing functions that could result in improved diagnosis and fewer repeated examinations. With the advent of electronic record systems, images can be stored in the computer memory and easily retrieved on the same computer screen and can be saved indefinitely or be printed on paper or film if necessary.

2. RELATED WORK:

MATLAB (matrix laboratory) is a multi-paradigm numerical computing environment and fourth-generation programming language. A proprietary programming language developed by Math Works, MATLAB allows matrix manipulations, plotting of functions and data, implementation of algorithms, creation of user interfaces, and interfacing with programs written in other languages, including C, C++, Java, Fortran and Python.Two main components for building an effective age estimator are facial feature extraction and estimator learning.A digital image is composed of pixels which can be thought of as small dots on the screen. A digital image is an instruction of how to color each pixel. We will see in detail later on how this is done in practice. A typical size of an image is 512-by-512 pixels. Later on in the course you will see that it is convenient to let the dimensions of the image to be a power of 2. For example, 2^9=512. In the general case we say that an image is of size m-by-n if it is composed of m pixels in the vertical direction and n pixels in the horizontal direction.Let us say that we have an image on the format 512-by-1024 pixels. This means that the data for the image must contain information about 524288 pixels, which requires a lot of memory! Hence, compressing images is essential for efficient image processing. You will later on see how Fourier analysis and Wavelet analysis can help us to compress an image significantly. There are also a few "computer scientific" tricks (for example entropy coding) to reduce the amount of data required to store an image.Moreover, in this work, we also empirically explored the importance of high-level nodule attributes such as calci cation, sphericity, lobulation and others to improve malignancy determination. Rather than manually determining these attributes we used 3D CNN to learn discriminative features corresponding to these attributes. The 3D CNN based features from these attributes are fused in a graph regularized sparse multi-task learning.

Another important imaging modality for lung nodule diagnosis is Positron Emission Tomography (PET). It has been found that the combination of PET and CT can improve the diagnostic accuracy of solitary lung nodules [22]. With the increase in the availability of PET/CT scanners, our future work will involve their utilization for simultaneous detection and characterization of pulmonary nodules.

3. PROPOSED SYSTEM:

Lung and Pancreatic cancers are the most common cancers in the world. They are the major cause of cancer-related deaths in the world. This work mainly focuses on the challenging problem of automatic diagnosis of Intraductal Papillary Mucinous Neoplasms (IPMN) found in the main pancreatic duct and its branches. This work uses two main approaches for tumor characterization from radiology scans: supervised and unsupervised learning algorithms for the diagnosis of lung nodules and IPMN. These works mainly focus on the challenging problem of automatic diagnosis of lung and pancreatic cancers from MRI

scans. Used in medical image analysis. For lung nodule characterization, a 3D CNN based supervised learning approach is proposed

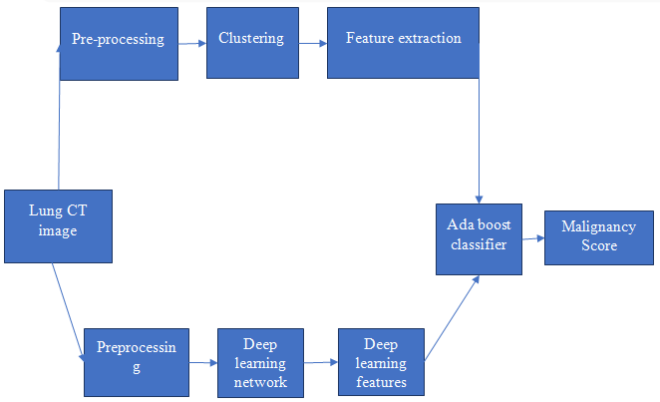

Fig. 3 Block Diagram of Proposed System

A fine-tuning strategy is used to avoid the requirement for a large number of volumetric training examples for 3D CNN. For this purpose, a pre-trained network (which is trained on 1 million videos) is used and fine-tune it on the CT data. A graph regularized sparse MTL platform to integrate the complementary features from lung nodule attributes is introduced so as to improve malignancy prediction.Evaluate the proposed supervised and unsupervised learning algorithms to determine the characterization of lung nodules and IPMN cysts.Thisis the first work to investigate the automatic diagnosis of IPMNs from MRI.In the proposed unsupervised learning algorithm, instead of hard assigning labels, we estimate the label proportions in a data-driven manner. Additionally, to alleviate the effect of noisy labels (i.e. mislabels) obtained during clustering, we propose to employ ∝SVM, which is trained on label proportions only. Some of the primary advantages that we have got from our proposed system are listed below.

- Automatic diagnosis of IPMNs from MRI.
- Regression accuracy and mean absolute score difference for lung nodule characterization of the Proposed 3D CNN with Multi-task Learning is 91.26% and 0.456.
- Average classification accuracy, sensitivity, and specificity of the proposed unsupervised approach for IPMN are 58.04%, 58.61%, 41.67% and 78.06% respectively and for lung nodule classification are 78.06%, 77.85% and 78.28% respectively.

Problem Formulation

Let $X = [x_1; x_2 : : : x_n]^T$ 2 $R^{n\,d}$ represent the input features obtained from n images of lung nodules each having a dimension d. Each data sample has an attribute/malignancy score given by $Y = [y_1; y_2 : : : y_n]$, where $Y^{\,T}$ 2 R^{n1}. While X consists of features extracted from radiology images, and represents the malignancy score over 1-5 scale where 1 represents benign and 5 represents malignant. In supervised learning, the labeled training data is used to learn the coefficient vector or the regression estimator W 2 R^d. In testing, W is used to estimate Y for an unseen feature/example. For regression, a regularizer is often added to prevent over-fitting. Hence, a classical least square regression turns into a constrained optimization problem with $'_1$ regularization as:

In the above equation, the sparsity level of the coefficient vector $W = [w_1; w_2 : : : w_d]$ is controlled by a parameter t. Since the function in Eq. (1) is convex and the constraints define a convex set, a local minimizer of the objective function is subjected to constraints corresponding to a global minimizer. In the following subsections, we extend this supervised learning setting with deep learning and MTL concepts to characterize lung nodules as benign or malignant.

3D Convolution Neural Network (CNN) and Fine-Tuning

We use 3D CNN [33] trained on Sports-1M dataset [34] and fine-tune it on the lung nodule CT dataset. The Sports-1M dataset consists of 487 classes with 1 million videos. As the lung nodule dataset doesn't have a large number of training examples, fine-tuning is done to acquire dense feature representation from the Sports-1M. The 3D CNN architecture consists of 5 sets of convolution, 2 fully-connected and 1 soft-max classification layers. Each convolution set is followed by a max-pooling layer. The input to the 3D CNN comprises dimensions of 128x171x16, where 16 denote the number of slices. Note that the images in the dataset are resized to have consistent dimensions such that the number of channels is 3 and the number of slices is fixed to 16. Hence, the overall input dimension can be considered as 3x16x128x171. The number of filters in the

first 3 convolution layers are 64, 128 and 256 respectively, whereas there are 512 filters in the last 2 layers. The fully-connected layers have a dimension 4096 which is also the length of feature vectors used as an input to the MTL framework. Implementation details are mentioned in section V-C.

Multi-Task Learning (MTL)

Multi-task learning is an approach of learning multiple tasks simultaneously while considering disparities and similarities across those tasks. Given M tasks, the goal is to improve the learning of a model for task i, (i 2 M) by using the information contained in the M tasks. We formulate the malignancy prediction of lung nodules as an MTL problem, where visual attributes of lung nodules are considered as distinct tasks (Figure 2A). In a typical MTL problem, initially, the correlation between M tasks and the shared feature representations are not known. The aim in the MTL approach is to learn a joint model while exploiting the dependencies among visual attributes (tasks) in feature space. In other words, we utilize visual attributes and exploit their feature level dependencies so as to improve regressing malignancy using other attributes.

As shown in Figure 2B, we design lung tumor characterization as an MTL problem, where each task has model parameters W_i, which are utilized to characterize the corresponding task i. When $W = [W_1; W_2 : : : W_M] \; 2 \; R^{d \; M}$ constitutes a rectangular matrix, rank can be considered as a natural extension to cardinality, and nuclear/trace norm leads to low rank solutions. In some cases nuclear norm regularization can be considered as the '1-norm of the singular values. Trace norm, the sum of singular values, is the convex envelope of the rank of a matrix (which is non-convex), where the matrices are considered on a unit ball. After substituting, '1-norm by trace norm, the least square loss function with trace norm regularization can be formulated as:

As the task relationships are often unknown and are learned from data, we represent tasks and their relations in the form because the '1norm is not differentiable at W = 0 and gradient descent approach fails to provide sparse solutions. Since the optimization function in the above equation has both smooth and non-smooth convex parts, it can be solved after replacing the non-smooth part with its estimates. In other words, the '1-norm in the above equation is the non-smooth part and the proximal operator can be used for its estimation. For this purpose, we utilize accelerated proximal gradient method, the first order gradient method having a convergence rate of O (1=m2), where m controls the number of iterations.

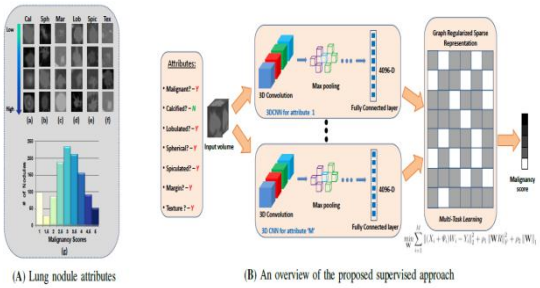

(A) Lung nodule attributes (B) An overview of the proposed supervised approach

Figure 4: (A) A visualization of lung nodules having different levels of attributes. On moving from the top (attribute absent) to the bottom (attribute prominently visible), the prominence level of the attribute increase. Different attributes including calcification, sphericity, margin, lobulation, spiculation and texture can be seen in (a-f). The graph in (g) depicts the number of nodules with different malignancy levels in our experiments using the publicly available dataset [32]. An overview of the proposed 3D CNN based graph regularized sparse MTL approach is presented in (B).

UNSUPERVISED LEARNING METHODS

Since annotating medical images is laborious, expensive and time-consuming, in the second part of this paper, we explore the potential of unsupervised learning approaches for tumor characterization problems. As illustrated in Figure 3, our proposed unsupervised framework includes three steps. First, we perform clustering on the appearance features obtained from the images to estimate an initial set of labels. Then, using the obtained initial labels, we compute label proportions corresponding to each cluster. Finally, we use the initial cluster assignments and label proportions to learn the categorization of tumors.

Initial Label Estimation

Let X = [x1; x2 : : : xn]T 2 Rn_d represent the input matrix which contains features from n images such that x 2 Rd. We then cluster the data into 2 _ k < n clusters using k-means algorithm. Let A represent jXj _ k assignment matrix which denotes the membership assignment of each sample to a cluster.

Learning with the Estimated Labels

Since our initial label estimation approach is unsupervised, there are uncertainties associated with them. It is, therefore, reasonable to assume that learning a discriminative model based on these noisy instance level labels can deteriorate classification performance. In order to address this issue, we model the instance level labels as latent variables and thereby consider group/bag level labels. Inspired by /SVM approach, which models the latent instance level variables using the known group level label proportions, we formulate our learning problem such that clusters are analogous to the groups. In our formulation, each cluster v can be represented as a group such that the majority of samples belong to the class v.

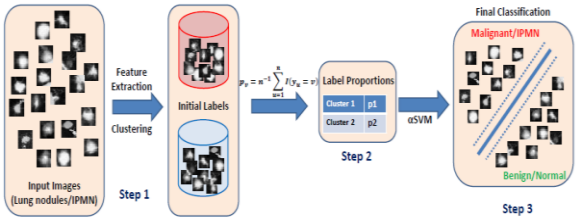

Figure 5: An outline of the proposed unsupervised approach. Given the input images, we compute GIST features and perform k-means clustering to get the initial set of labels which can be noisy. Using the set of labels, we compute label proportions corresponding to each cluster/group. We finally employ SVM to learn a discriminative model using the features and label proportions.Considering the groups to be disjoint such that Sk v=1v= 1; 2; : : : n , and represents groups; the objective function of the large-margin /SVM after convex relaxation can be formulated.

A.AdaBoost classifier

Boosting is another state-of-the art model that is being used by many data scientists to win so many competitions. In this section, we will be covering the **AdaBoost** algorithm, followed by **gradient boost** and **extreme gradient boost (XGBoost).** Boosting is a general approach that can be applied to many statistical models. However, in this book, we will be discussing the application of boosting in the context of decision trees. In bagging, we have taken multiple samples from the training data and then combined the results of individual trees to create a single predictive model; this method runs in parallel, as each bootstrap sample does not depend on others. Boosting works in a sequential manner and does not involve bootstrap sampling; instead, each tree is fitted on a modified version of an original dataset and finally added up to create a strong classifier:

4. EXPERIMENTAL RESULTS AND DISCUSSION:

For our experimental result, we have used a scanned lung image to produce the results for our work. In this work, using this lung image we have gone through supervised and unsupervised algorithms and brought up with the results successfully. The various images obtained via the input image given into the classifier shows the expected accuracy level of the Ada-boost classifier and simply proves that this algorithm used is the best way to characterize the tumors in early stage itself

Fig.(a)

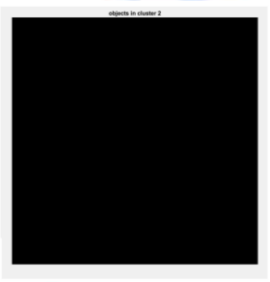

Fig.(b)

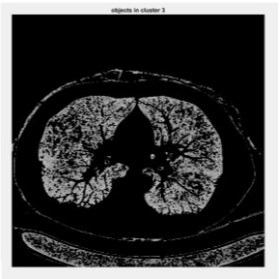

Fig.(c)

Fig.(d)

The above listed images are the images formed through the process of clustering. Image segmentation plays a very important role in image processing. This image segmentation results in bringing out the similar objects in an image. Clustering plays the major role in this image segmentation. Clustering is a process of separation of an image data set into disjoint groups and clusters. Clustering is an important part in the Ada-boost algorithm in deep learning approach. In Ada-boost algorithm, the process happens multiple numbers of times and this result in extraction of similar objects in an image data set. As said earlier, iteration happens till the completion of extraction of the image

clusters. Fig (a) is the initiation of iteration process. Here, the clustering takes place and at the end of iteration, the image labelled by the cluster index is placed in fig. (d).

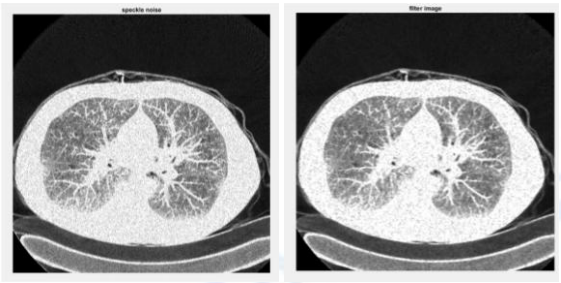

Fig.(e) **Fig.(f)**

The image processing goes through a vital phase ie.,removal of noise by filtering.This project work involves the removal of speckle noise. A noise detector is used in finding out the presence of noise in an image. There are many number of noises in image processing. One of those is speckle noise fig.(e). Speckle noise occurs due to the interference of sound waves in the dataset. It occurs in granular pattern and in multiplicative form. By undergoing speckle filtering, we have to reduce the variance value and improve the mean value of the sample. As a result, filtering removes the granular noise pattern and this gives the filtered image in fig.(f).

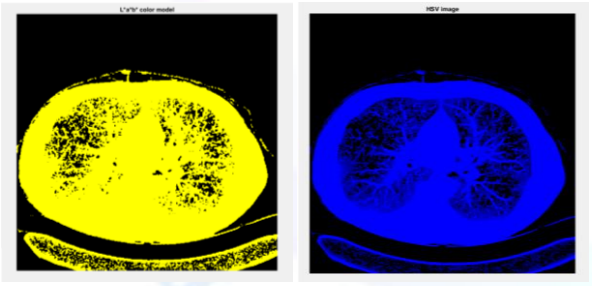

Fig.(g) **Fig.(h)**

Conflict of interest statement

Authors declare that they do not have any conflict of interest.

REFERENCES

[1] Society, A.C.: Cancer Facts & Figures. American Cancer Society (2016)

[2] Sadot, E., Basturk, O., Klimstra, D.S., Gonen,¨ M., Anna, L., Do, R.K.G., DAngelica, M.I., DeMatteo, R.P., Kingham, T.P., Jarnagin, W.R., et al.: Tumor-associated neutrophils and malignant progression in intraductal papillary mucinous neoplasms: an opportunity for identification of high-risk disease. Annals of surgery 262(6), 1102 (2015)

[3] El-Baz, A., Nitzken, M., Khalifa, F., Elnakib, A., Gimelfarb, G., Falk, R., El-Ghar, M.A.: 3D shape analysis for early diagnosis of malignant lung nodules. In: IPMI. pp. 772–783. Springer (2011)

[4] Han, F., Wang, H., Zhang, G., Han, H., Song, B., Li, L., Moore, W., Lu, H., Zhao, H., Liang, Z.: Texture feature analysis for computer-aided diagnosis on pulmonary nodules. Journal of Digital Imaging 28(1), 99– 115 (2015)

[5] Way, T.W., Hadjiiski, L.M., Sahiner, B., Chan, H.P., Cascade, P.N., Kazerooni, E.A., Bogot, N., Zhou, C.: Computer-aided diagnosis of pulmonary nodules on CT scans: segmentation and classification using 3D active contours. Medical Physics 33(7), 2323–2337 (2006)

[6] Lee, M., Boroczky, L., Sungur-Stasik, K., Cann, A., Borczuk, A., Kawut, S., Powell, C.: Computer-aided diagnosis of pulmonary nodules using a two-step approach for feature selection and classifier ensemble construction. Artificial Intelligence in Medicine 50(1), 43–53 (2010)

[7] Kumar, D., Wong, A., Clausi, D.A.: Lung nodule classification using deep features in CT images. In: Computer and Robot Vision (CRV), 2015 12th Conference on. pp. 133–138. IEEE (2015)

[8] Buty, M., Xu, Z., Gao, M., Bagci, U., Wu, A., Mollura, D.J.: Characterization of Lung Nodule Malignancy Using Hybrid Shape and Appearance Features. In: MICCAI. pp. 662–670. Springer (2016)

[9] Saouli, R., Akil, M., Kachouri, R., et al.: Fully automatic brain tumor segmentation using end-to-end incremental deep neural networks in mri images. Computer methods and programs in biomedicine 166, 39–49 (2018)

[10] Hussein, S., Cao, K., Song, Q., Bagci, U.: Risk Stratification of Lung Nodules Using 3D CNN-Based Multi-task Learning. In: International Conference on Information Processing in Medical Imaging. pp. 249– 260. Springer (2017)

[11] Furuya, K., Murayama, S., Soeda, H., Murakami, J., Ichinose, Y., Yauuchi, H., Katsuda, Y., Koga, M., Masuda, K.: New classification of small pulmonary nodules by margin characteristics on highresolution CT. Acta Radiologica 40(5), 496–504 (1999)

[12] Uchiyama, Y., Katsuragawa, S., Abe, H., Shiraishi, J., Li, F., Li, Q., Zhang, C.T., Suzuki, K., Doi, K.: Quantitative computerized analysis of diffuse lung disease in high-resolution computed tomography. Medical Physics 30(9), 2440–2454 (2003)

[13] Chen, S., Ni, D., Qin, J., Lei, B., Wang, T., Cheng, J.Z.: Bridging computational features toward multiple semantic features with multi-task regression: A study of

CT pulmonary nodules. In: MICCAI. pp. 53–60. Springer (2016)
[14] Shen, W., Zhou, M., Yang, F., Yang, C., Tian, J.: Multi-scale convolutional neural networks for lung nodule classification. In: IPMI. pp. 588–599. Springer (2015)
[15] Ciompi, F., Chung, K., Van Riel, S.J., Setio, A.A.A., Gerke, P.K., Jacobs, C., Scholten, E.T., Schaefer-Prokop, C., Wille, M.M., Marchiano,` A., et al.: Towards automatic pulmonary nodule management in lung cancer screening with deep learning. Scientific reports 7, 46479 (2017)
[16] Setio, A.A.A., Ciompi, F., Litjens, G., Gerke, P., Jacobs, C., van Riel, S.J., Wille, M.M.W., Naqibullah, M., Sanchez,´ C.I., van Ginneken, B.: Pulmonary nodule detection in CT images: false positive reduction using multi-view convolutional networks. IEEE TMI 35(5), 1160–1169 (2016)
[17] Setio, A.A.A., Traverso, A., De Bel, T., Berens, M.S., van den Bogaard, C., Cerello, P., Chen, H., Dou, Q., Fantacci, M.E., Geurts, B., et al.: Validation, comparison, and combination of algorithms for automatic detection of pulmonary nodules in computed tomography images: the luna16 challenge. Medical image analysis 42, 1–13 (2017)
[18] Khosravan, N., Bagci, U.: S4ND: Single-Shot Single-Scale Lung Nodule Detection. arXiv preprint arXiv:1805.02279 (2018)
[19] Zhou, Y., Xie, L., Fishman, E.K., Yuille, A.L.: Deep Supervision for Pancreatic Cyst Segmentation in Abdominal CT Scans. arXiv preprint arXiv:1706.07346 (2017)
[20] Cai, J., Lu, L., Zhang, Z., Xing, F., Yang, L., Yin, Q.: Pancreas segmentation in MRI using graph-based decision fusion on convolutional neural networks. In: MICCAI. pp. 442–450. Springer (2016)
[21] Hanania, A.N., Bantis, L.E., Feng, Z., Wang, H., Tamm, E.P., Katz, M.H., Maitra, A., Koay, E.J.: Quantitative imaging to evaluate malignant potential of IPMNs. Oncotarget 7(52), 85776 (2016)
[22] Gazit, L., Chakraborty, J., Attiyeh, M., Langdon-Embry, L., Allen, P.J., Do, R.K., Simpson, A.L.: Quantification of CT Images for the Classification of High-and Low-Risk Pancreatic Cysts. In: SPIE Medical Imaging. pp. 101340X–101340X. International Society for Optics and Photonics (2017)
[23] Sivic, J., Russell, B.C., Efros, A.A., Zisserman, A., Freeman, W.T.: Discovering objects and their location in images. In: ICCV. vol. 1, pp. 370–377. IEEE (2005)
[24] Kamper, H., Jansen, A., Goldwater, S.: Fully unsupervised small-vocabulary speech recognition using a segmental Bayesian model. In: Interspeech (2015)
[25] Lee, H., Pham, P., Largman, Y., Ng, A.Y.: Unsupervised feature learning for audio classification using convolutional deep belief networks. In: Advances in neural information processing systems. pp. 1096–1104 (2009)
[26] Shin, H.C., Orton, M.R., Collins, D.J., Doran, S.J., Leach, M.O.: Stacked autoencoders for unsupervised feature learning and multiple organ detection in a pilot study using 4d patient data. IEEE transactions on pattern analysis and machine intelligence 35(8), 1930–1943 (2013)
[27] Vaidhya, K., Thirunavukkarasu, S., Alex, V., Krishnamurthi, G.: Multi-modal brain tumor segmentation using stacked denoising autoencoders. In: International Workshop on Brainlesion: Glioma, Multiple Sclerosis, Stroke and Traumatic Brain Injuries. pp. 181–194. Springer (2015)
[28] Sivakumar, S., Chandrasekar, C.: Lung nodule segmentation through unsupervised clustering models. Procedia engineering 38, 3064–3073 (2012)
[29] Kallenberg, M., Petersen, K., Nielsen, M., Ng, A.Y., Diao, P., Igel, C., Vachon, C.M., Holland, K., Winkel, R.R., Karssemeijer, N., et al.: Unsupervised deep learning applied to breast density segmentation and mammographic risk scoring. IEEE transactions on medical imaging 35(5), 1322–1331 (2016)
[30] Radford, A., Metz, L., Chintala, S.: Unsupervised representation learning with deep convolutional generative adversarial networks. arXiv preprint arXiv:1511.06434 (2015)
[31] Zhang, F., Song, Y., Cai, W., Zhou, Y., Fulham, M., Eberl, S., Shan, S., Feng, D.: A ranking-based lung nodule image classification method using unlabeled image knowledge. In: IEEE ISBI. pp. 1356–1359. IEEE (2014)
[32] Armato III, S., McLennan, G., Bidaut, L., McNitt-Gray, M.F., Meyer, C.R., Reeves, A.P., Zhao, B., Aberle, D.R., Henschke, C.I., Hoffman, E.A., et al.: The Lung Image Database Consortium (LIDC) and Image Database Resource Initiative (IDRI): a completed reference database of lung nodules on CT scans. Medical Physics 38(2), 915–931 (2011)
[33] Tran, D., Bourdev, L., Fergus, R., Torresani, L., Paluri, M.: Learning spatiotemporal features with 3D convolutional networks. In: ICCV. pp. 4489–4497. IEEE (2015)
[34] Karpathy, A., Toderici, G., Shetty, S., Leung, T., Sukthankar, R., Fei-Fei, L.: Large-scale video classification with convolutional neural networks. In: IEEE CVPR. pp. 1725–1732 (2014)
[35] Recht, B., Fazel, M., Parrilo, P.A.: Guaranteed minimum-rank solutions of linear matrix equations via nuclear norm minimization. SIAM review 52(3), 471–501 (2010)
[36] Zhou, J., Chen, J., Ye, J.: MALSAR: Multi-task learning via structural regularization (2012)

[37] Shalev-Shwartz, S., Tewari, A.: Stochastic methods for l1-regularized loss minimization. Journal of Machine Learning Research 12(Jun), 1865–1892 (2011)
[38] Nesterov, Y.: Introductory lectures on convex optimization: A basic course, vol. 87. Springer Science & Business Media (2013)
[39] Yu, F., Liu, D., Kumar, S., Tony, J., Chang, S.F.: /SVM for Learning with Label Proportions. In: Proceedings of The 30th International Conference on Machine Learning. pp. 504–512 (2013)
[40] Tustison, N.J., Avants, B.B., Cook, P.A., Zheng, Y., Egan, A., Yushke-vich, P.A., Gee, J.C.: N4ITK: Improved N3 bias correction. IEEE Transactions on Medical Imaging 29(6), 1310–1320 (2010)
[41] Oliva, A., Torralba, A.: Modeling the shape of the scene: A holistic representation of the spatial envelope. IJCV 42(3), 145–175 (2001)
[42] Chatfield, K., Simonyan, K., Vedaldi, A., Zisserman, A.: Return of the devil in the details: Delving deep into convolutional nets. In: British Machine Vision Conference (2014)
[43] He, H., Bai, Y., Garcia, E.A., Li, S.: ADASYN: Adaptive synthetic sampling approach for imbalanced learning. In: Neural Networks, 2008. IJCNN 2008.(IEEE World Congress on Computational Intelligence). IEEE International Joint Conference on. pp. 1322–1328. IEEE (2008)
[44] Kalb, B., Sarmiento, J.M., Kooby, D.A., Adsay, N.V., Martin, D.R.: MR imaging of cystic lesions of the pancreas. Radiographics 29(6), 1749– 1765 (2009)
[45] Ma, L., Lu, Z., Shang, L., Li, H.: Multimodal convolutional neural networks for matching image and sentence. In: IEEE ICCV. pp. 2623– 2631 (2015)
[46] Nguyen, A., Yosinski, J., Bengio, Y., Dosovitskiy, A., Clune, J.: Plug & play generative networks: Conditional iterative generation of images in latent space. arXiv preprint arXiv:1612.00005 (2016)
[47] Larsen, A.B.L., Sønderby, S.K., Larochelle, H., Winther, O.: Auto encoding beyond pixels using a learned similarity metric. In: ICML (2016)
[48] Springenberg, J.T.: Unsupervised and semi-supervised learning with categorical generative adversarial networks. arXiv preprint arXiv:1511.06390 (2015)
[49] Chen, X., Duan, Y., Houthooft, R., Schulman, J., Sutskever, I., Abbeel, P.: Infogan: Interpretable representation learning by information maxi-mizing generative adversarial nets. In: Advances in Neural Information Processing Systems. pp. 2172–2180 (2016)